

Robust Fuzzy C-Means Cluster Algorithm through Energy Minimization for Image Segmentation

T. V. Sai Krishna¹ and A. Yesu Babu² and A. Ananda Rao³

¹Department of Computer Science and Engineering JNTU, Kakinada, Jawaharlal Nehru Technological University Road, Kakinada - 533003, Andhra Pradesh, India; tvsai.kris@gmail.com

²Department of Computer Science and Engineering Sir CRR College of Engineering, Valturu Post Peddapadu Mandal, Near Bypass Road, West Godavari District, Eluru - 534007, Andhra Pradesh, India; adimulam9@gmail.com

³Director Academic and Planning, JNTUA, Anantapur – 515002, Andhra Pradesh, India

Abstract

Background: The Fuzzy c-means (FCMCA) cluster algorithm with spatial information is adopted for image segmentation. In the direction of acceptable segmentation concert on noisy images, the anticipated technique exemplifies the foreign spatial evidence derived from the image and also inherits appropriateness which correspondingly reflects on the universal fuzzy fitness and fuzzy isolation among the clusters. **Methods:** Segmentation combines two regions firstly, the physical dimension of the image and contextual data through energy reduction function. Secondly, since the kernel metric value is merged with fuzziness of the energy level, the dynamic delineation progresses is steadily deprived of the reinitialization progress for the level set process. Afterwards generating the bunch of non-conquered clarifications, the concluding clustering elucidation is preferred through Cluster Validity Index (CVI) by consuming the foreign spatial evidence. Additionally, the total number of clusters incorporates the actual oblique mutable string length scheme to encrypt the cluster groups in terms of grouped chromosomes spontaneously. **Findings:** This novel fuzzy and nonlinear type of energy functionality brands the modernizing of region group's added strength against the noise and edge of the image. The projected method is undergone with image polluted through noise and likened with fuzzy c & k means, dual FCM cluster based approaches with predefined spatial data and dynamic string size is inherited by fuzzy clustering procedure. **Applications/Improvements:** The investigational outcome demonstrates that the anticipated technique performs thriving in developing the sum of clusters and procurement in acceptable performance on noise in image segmentation process.

Keywords: Chan-Vese Model, Cluster Validity Index (CVI), Foreign Spatial Evidence, Fuzzy c & k-means Clustering, Image Segmentation

1. Introduction

The Image segmentation (IS) is predominantly essential with significant task in computer vision and artificial trending mechanisms. There are numerous approaches for image segmentation have been anticipated for example thresholding¹, Image clustering², Image edge finding and so on. Nevertheless, because of existence of noise and minimal contrast and pixels in images, outliers. Amongst these approaches, an entrenched set of procedures like

active contour models (ACMs). It has dual merits over conventional approaches stated above. This could be attain improved accurateness in segmentation³ expressed as a minimalist through energy function that permits the amalgamation of diverse and beneficial image material⁴⁻⁶. Moreover ACM is initially recognized as a snake model projected by the author Kass et al⁷. Through the growth of active contour practice, diverse distinctions of ACM's consumed and anticipated for IS. Conferring to the variable necessities pouring the advancement, prevailing

*Author for correspondence

ACM's could be approximately placed into two nominal classes: Region-based Mmodels (RBM)¹¹⁻¹⁴ and Edge-based models (EBM)^{3,8-10}.

2. Related Works

One of the greatest well-known and extensively used RBM are Chan–Vese (CV) model¹¹ that is depends with Mumford–Shah functionality which anticipated by T. F. Chan et al.¹⁵. This approach make use of the global intensity variance among the host image and its difference image to direct delineation. The difference image is fabricated under the supposition that the intensity are remain constant of the original image through CV model. Moreover this approach is very effective to spot the objects of which the limits are not certainly distinct by gradient. Nevertheless, on other hand the sign distance function^{16,17} is utilized as the original LSF on CV might be extremely ruined through the progression. Typically this practice is referred as reinitialization of LSF. This deployed intermittently to reserve the distance figures of the LSF and preserve the steadiness of progression.

A suitable technique to discard local ideality to build a bi-convex method by presenting fuzzy group sets²⁰. Fuzzy sets is tends to consume general approach on image segmentation and data clustering which is articulated by S. Krinidis & V. Chatzis²¹. By merging the fuzzy clusters and dynamic delineation procedure, the fuzzy energy-based active contour (FEBAC) method projected in²¹ has a capability of refusing local bits. This method is expressed through a pseudo-level grouping function, the active delineation is characterized through the 0.5 level set of LSF that likewise termed as fuzzy membership function. Besides as an alternative of classical approaches resolving Euler–Lagrange equation, a straight technique depend on a rapid optimization process anticipated by B. Song and T. Chan²² is realistically to reduce the fuzzy energy function. Subsequently the conjunction of this prototypical could be attained after identical repetitions and the computational rapidity is fair. In the meantime, this prototypical approach not requires the reinitialization progression and the detachment normalized term is not amalgamated in energy function^{23,24}. Nevertheless, for pictures without maximum contrast, this prototypical approach may produce without decent equilibrium among stability and efficiency²⁵⁻²⁷.

There are many investigators familiarized the three-dimensional evidence to derivative relative pixel in the specified image into the concluding objective function of FCM method^{28,33-36}. This is for the unique purpose of reducing the secrecy level of FCM to the noise ratio with real image. Ahmed et al.³³ adapted the unbiased method of FCM by integrating nearest spatial locality factor and anticipate FCM approach by including spatial locality information (FCM-S). Consequently, Chen and Zhang²⁸ proposed two alternatives of FCM Spatial¹ and FCM Spatial² to minimize the computational difficulty of FCM-S. Additionally, in ref.^{29,30}, author exploited a kernel-based detachment to standby the Euclidean detachment and offered the kernel versions of FCM Spatial¹ and FCM Spatial². To facilitate hasten in the image segmentation procedure of FCM including spatial information, Szilagyi et al.³⁴ produced a linearly-weighted quantity duplicate image and projected a superior fuzzy c-means clustering procedure (EnFCM). Subsequently the gray level histogram takes place on engendered quantity of image in place of the individual pixels. This is comparable to EnFCM, Cai et al.³⁶ author Zhao et al.³⁷ familiarized a foreign spatial evidence resultant from a large image m and build the spatial restriction tenure (FCM-NLS). Although the foreign spatial evidence of any individual pixel is attained by exploiting and comparable formation of the specified pixel^{31,32,38,39}.

3. The Chan_Vese (CV) Model

The Chan–Vese (CV) model¹⁹ is articulated through minimizing an energy function by the Mumford–Shah (MS) model. This model fabricates agility against noise factor. The fundamental notion of MS model is to discover an original image I_{Ori} using to approximated image I_{App} . In this formation the edge E which fragments the original host image into non-overlying sections of given image Γ . The basic energy level function of MS model¹⁵ can be well-defined by Equation 1.

$$MS(I, E) = \int (I_{Ori}(x) - I_{App}(x)) dx + \int_{\Gamma/E} |\tilde{\nabla} I_{App}(x)|^2 dx + \omega \cdot Len(E) \dots \dots \dots 1$$

Such that $\tilde{\nabla}$ is known as gradient operator. In this equation the first segment defines the mean square data

term subsequently the second segment shows normalizing term which tends to deploy smooth portions. The final segment modernize the edge set E to be normalized. In some special case, the intensities in the estimated image I will remain constant. This occasion is known as the cartoon limit by which the second segment fulfills

$\int_{\Gamma/E} |\tilde{\nu} I_{App}(x)|^2 dx = 0$. Predominantly, in the state of two stage segmentation, the image Γ could be diverse into dual mirrored regions: inside (E) and outside (\bar{E}) represented with single constant. However the other two constants e_I and e_O to characterize the intensity averages of I_{Ori} both inside and outside. Henceforth, the energy formation of CV model¹¹ is expressed by Equation 2,

$$CV(e_I, e_O, E) = \omega \cdot Len(E) + \Delta_1 \int_{e_I} |I_{ori}(x) - e_I|^2 dx + \Delta_2 \int_{e_O} |I_{ori}(x) - e_O|^2 dx \quad \text{-----} 2$$

Here Δ_1 and Δ_2 are constant parameters and typically both will set to 1. The level set methodology were introduced to minimize the energy function in Equation 2, and the edge E will get evolved, so that it is denoted as the zero level significance of the LSF (ψ) consequently it is represented as,

$$\begin{cases} E = (x \in \Gamma : \psi(x) = 0) \\ e_I = (x \in \Gamma : \psi(x) > 0) \\ e_O = (x \in \Gamma : \psi(x) < 0) \end{cases} \quad \text{-----} 3$$

Thus, the energy formation could be stated in addition with Equation 3

$$CV = (e_I, e_O, E) = \omega \cdot \int_{\Gamma} \gamma(\psi(x)) |\tilde{\nu} \psi(x)| dx + \Delta_1 \int_{\Gamma} |I_{Ori}(x) - e_I|^2 K(\psi(x)) dx + \Delta_2 \int_{\Gamma} |I_{Ori}(x) - e_O|^2 (1 - K(\psi(x))) dx \quad \text{-----} 4$$

And the Heaviside K and Dirac γ could be expressed through Equation 4

$$K(x) = \begin{cases} 1 & x \geq 0 \\ 0 & x < 0 \end{cases} \quad \lambda(x) = \frac{d}{dx}(K(x)) \quad \text{-----} 5$$

The energy level formation in equation 5 is reduced by calculating related EL and steepest procedure to modernize the LSF. Based on implantation of region data, the CV model is become more agile against noise and very effective in perceiving weak limitations which are certainly sharp by gradient parameter.

4. Fuzzy Dynamic Delineation Model (FDDM)

The FDDM model is region-based prototype model which syndicates the fuzzy group sets with the dynamic delineation formation. This model is slightly vary with CV model, the progressing delineation is indirectly signified as the 0.5 zero level set of the LSFF_M, by which it is represented in equation 5.

$$\begin{cases} E = (x \in \Gamma : F_M(x) = 0.5) \\ e_I = (x \in \Gamma : F_M(x) > 0.5) \\ e_O = (x \in \Gamma : F_M(x) < 0.5) \end{cases} \quad \text{-----} 6$$

$$F_E(E, e_I, e_O, F_M) = \omega \cdot Len(E) + \Delta_1 \int_{\Gamma} (F_M(x))^t (I_{Ori}(x) - e_I)^2 dx + \Delta_2 \int_{\Gamma} (1 - F_M(x))^t (I_{Ori}(x) - e_O)^2 dx \quad \text{-----} 7$$

The function F_M is referred as fuzzy membership function. $F_M(x)$ describes the membership constant with the pixel x fits into e_I and $1 - F_M(x)$ signifies the membership constant with pixel x fits to e_O . The member function t typically dual with the weighting proponent on both fuzzy membership. The e_I & e_O are mid models of the origin image inside E and outside E . With the constant factor F_M , the reduction of energy functions in equation 2 based on e_I & e_O . Through which it is feasible to attain the possible formation to update e_I & e_O . The corresponding equations are defined through Equation 8 and equation 9.

$$e_I = \frac{\int_{\Gamma} (F_M(x))^t I_{Ori}(x) dx}{\int_{\Gamma} (F_M(x))^t dx} \quad \text{-----} 8$$

$$e_O = \frac{\int_{\Gamma} (1 - F_M(x))^t I_{Ori}(x) dx}{\int_{\Gamma} (1 - F_M(x))^t dx} \quad \text{-----} 9$$

The e_i & e_o are stable and the length term sustainability, we minimize the energy formation in equation 7 with respect to F_M , without dropping the generalization, the equation used to update F_M is defined by equation 10.

$$F_M = \frac{1}{1 + \left(\frac{\Delta_1(I_{Ori}(x) - e_i)^2}{\Delta_2(I_{Ori}(x) - e_o)^2} \right)^{\frac{1}{t-1}}} \quad \text{--- 10}$$

Precisely, for a particular pixel x_i , to calculate the novel fuzzy membership function using equation 10, there should be stability in understanding the change which is triggered by the particular alteration with fuzzy membership on the pixel x_i . Subsequently if there is any change in F_E then it makes F_E convert into smaller ($\Delta F_E < 0$), finally the new fuzzy membership will be fabricated. In case of no substantial change on old formation is taken for consideration⁴⁶. Moreover, conferring to the updating principle of F_M , pixels background might be simply tagged as like pixels which owned by object region space, only if current intensities are identical with the object region.

A. Energy Level Construction

In these models designated above, the space $(I_{Ori} - E)^2$ and $C = (e_i, e_o)$ is to paradigm image data in terms of energy level formulation. This cadenced process tends to lead non-robust image segmentation outcome of given images with stipulated noise. As formulated in equation (8) and (9) is for respective pixel x_i , it is perceptible that the modernizing of average patterns can be inclined by the original intensity ratio $I_{Ori}(x_i)$ when it is outline scope. In order to minimize the consequence of noise and outline scope for a strong breakdown, we substitute the L_2 normalization along with nonlinear form of space constant.

The kernel scheme is extensively realistic in fabricating a nonlinear structure of a linear procedure. Provided this scheme could also suit an inactive delineation procedure. A mutual kernel distance metric constant could be briefly articulated through equation (11).

$$K_M = (\alpha_1, \alpha_2) = \{\Theta(\alpha_1), \Theta(\alpha_2)\} = \Theta(\alpha_1)^T \Theta(\alpha_2) -$$

Where the α_1 & α_2 are two vectors having the similar dimension. The $\Theta(\cdot)$ represents a nonlinear flow and $\{\Theta(\alpha_1), \Theta(\alpha_2)\}$ signifies the internal product process.

The Gaussian radial basis function (GRBF) is a broadly applied in kernel process and the customized version of GRBF is implemented this presented work is affirmed by equation (12).

$$K_M = \exp\left(-\frac{(\alpha_1 - \alpha_2)^2}{\varpi}\right) \quad \text{--- (12)}$$

In this equation the parameter ϖ is signifies the bandwidth of the total kernel process and would be rapidly nominated by a defined rule clarified in the upcoming sections. The defined $K_M(\alpha_1, \alpha_1)$ is corresponding to 1. Formerly we paradigm the nonlinear space distance via equation (13) to substitute through Euclidean distance variations.

$$\begin{aligned} \|\Theta(\alpha_1) - \Theta(\alpha_2)\|^2 &= (\Theta(\alpha_1) - \Theta(\alpha_2))^T (\Theta(\alpha_1) - \Theta(\alpha_2)) \\ &= K_M(\alpha_1, \alpha_1) + K_M(\alpha_2, \alpha_2) \\ &\quad - 2K_M(\alpha_1, \alpha_2) = 2 - 2K_M(\alpha_1, \alpha_2) \quad \text{--- (13)} \end{aligned}$$

For ease simplification, we typically utilized the kernel distance variations as $\exists_{EK} (\exists_{EK} = 1 - K_M(\alpha_1, \alpha_2))$ to exchange the Euclidean distance $\exists_{EU} (\exists_{EU} = \|\alpha_1 - \alpha_2\|^2)$. Henceforth the nonlinear energy process integrating fuzzy sets that articulated in equation (14) with the quasi level set previously illustrated in Equation (6).

$$\begin{aligned} F_E(E, e_i, e_o, F_M) &= \omega \cdot Len(E) + \Delta_1 \int_{\Gamma} (F_M(x))^t (1 - K_M(I_{Ori}(x) - e_i)) dx \\ &\quad + \Delta_2 \int_{\Gamma} (1 - F_M(x))^t (1 - K_M(I_{Ori}(x) - e_o)) dx \quad \text{--- (14)} \end{aligned}$$

However the delineation is implicitly characterized as the 0.5 level through set of F_M and consequently, we consume following Equation (15).

$$\begin{aligned} Len(E) &= \int_{\Gamma} |\tilde{\nu} K(F_M(x) - 0.5)| dx \\ &= \int_{\Gamma} \gamma(F_M(x - 0.5)) |\tilde{\nu} F_M(x - 0.5)| dx \quad \text{--- (15)} \end{aligned}$$

Such that the process K and γ are described already in equation (4). By Combining equation (14) and Equation (15), the projected energy function is articulated by equation (16).

$$\begin{aligned} F_E(e_i, e_o, F_M) &= \omega \cdot \int_{\Gamma} \gamma(F_M(x - 0.5)) |\tilde{\nu} F_M(x - 0.5)| dx \\ &\quad + \Delta_1 \int_{\Gamma} (F_M(x))^t (1 - K_M(I_{Ori}(x) - e_i)) dx \\ &\quad + \Delta_2 \int_{\Gamma} (1 - F_M(x))^t (1 - K_M(I_{Ori}(x) - e_o)) dx \quad \text{--- (16)} \end{aligned}$$

The straight minimization method used in FDDM process is not appropriate for this nonlinear energy functionality (16). It could be demonstrated through particular modification of fuzzy membership function F_M in the defined pixel x_i , the alteration of F_E is a nonlinear alteration connected with the previous F_E . In subsequent section we will deliver the minimization practice for the anticipated energy functionality.

B. Energy Level Minimization

The functional value of F_M is much varied when it corresponds minimum value of F_E described in Equation (16). Henceforth the deployment of sharpest linear scheme is engaged to diminish the anticipated energy function on regards with F_M, e_I & e_O . Initially, the fuzzy membership functional F_M value is remain constant, then we reduce the quantity of F_E through equation (16) based on e_I & e_O . Finally it is feasible to acquire the modernizing equations of e_I & e_O expressed by the equations (17 and 18).

$$e_I = \frac{\int_{\Gamma} (F_M(x))^t K_M(I_{Ori}(x), e_I) I_{Ori}(x) dx}{\int_{\Gamma} (F_M(x))^t K_M(I_{Ori}(x), e_I) dx} \text{-----} (17)$$

$$e_O = \frac{\int_{\Gamma} (1 - F_M(x))^t K_M(I_{Ori}(x), e_O) I_{Ori}(x) dx}{\int_{\Gamma} (1 - F_M(x))^t K_M(I_{Ori}(x), e_O) dx} \text{-----} (18)$$

It is perceptible that the section patterns e_I & e_O stagnant in the distance after modification. The distinctive that suggested energy origination is strong with noise and outline scope which can also attain by instinctive elucidation by equations (17) and (18). Each intensity $I_{Ori}(x)$ is capable with an added value of $K_M(I_{Ori}(x), \alpha)$ ($\alpha = \alpha_1, \alpha_2$) that possess the detachment by the original intensity $I_{Ori}(x)$ to typical prototype models. If the distance of the region prototype models is very extreme level in terms of their intensity and additional value of the related intensity is very minor. Therefore, for each single pixel x_i with the intensity $I_{Ori}(x)$ is an outlined and isolated from the region prototype models, the inspiration employed by $I_{Ori}(x)$ on the informing of region prototype models can be inhibited by the added value of $K_M(I_{Ori}(x), \alpha)$ in this given pixel. Formerly, when e_I & e_O are constant, we demise F_E in equation (16) based on F_M . Now the EL

equalities are engaged to build the undesirable gradient flow articulated as,

$$\begin{aligned} -\frac{\partial F_E}{\partial F_M} &= \omega \cdot \gamma(F_M(x) - 0.5) D_i \left(\frac{\tilde{\nabla}(F_M(x) - 0.5)}{|\tilde{\nabla}(F_M(x) - 0.5)|} \right) \\ &-\Delta_1 \cdot t \cdot (F_M(x))^{t-1} (1 - K_M(I_{Ori}(x), e_I)) \\ &+\Delta_2 \cdot t \cdot (1 - F_M(x))^{t-1} (1 - K_M(I_{Ori}(x), e_O)) \text{-----} (19) \end{aligned}$$

Such that $D_i(\bullet)$ is the divergence operator value. Laterally this undesirable gradient flow well-defined by equation (19), we diminish the energy function with equivalent F_M by an iterative scheme with simulated time t_i parameterizing the linear flow. Consequently, the minimization is again articulated by equations (20) and (21).

$$\begin{aligned} \frac{\partial F_M}{\partial t_i} - \frac{\partial F_E}{\partial F_M} &= \omega \cdot \gamma(F_M(x) - 0.5) D_i \left(\frac{\tilde{\nabla}(F_M(x) - 0.5)}{|\tilde{\nabla}(F_M(x) - 0.5)|} \right) \\ &-\Delta_1 \cdot t \cdot (F_M(x))^{t-1} (1 - K_M(I_{Ori}(x), e_I)) \\ &+\Delta_2 \cdot t \cdot (1 - F_M(x))^{t-1} (1 - K_M(I_{Ori}(x), e_O)) \text{-----} (20) \end{aligned}$$

$$F_M(0, x) = F_{M-Ori}(x) \text{ in } \gamma \text{-----} (21)$$

Where, $F_{M-Ori}(x)$ is the preliminary LSF and the Neumann boundary condition nominated to offer flexibility on implementation.

C. Classical FCM Algorithm

The FCMCA algorithm is process which permits a data origin point to fit single or multiple group clusters together. Consider an image represented as $A = \{a_1, a_2, \dots, a_x\}$ with x number of pixels, such that a_l signifies the gray value of corresponding l^{th} pixel. The core function of formal FCMCA algorithm is,

$$M = \sum_{N=1}^N \sum_{l=1}^x \int_{nl}^{em} p \|a_i - q_n\|^2 \text{-----} (22)$$

Such that q_n ($1 \leq n \leq N$) symbolizes the pixelated particles of the n^{th} cluster and consequently q_{nl} ($1 \leq n \leq N, 1 \leq l \leq x$) denotes the membership and association degree functional value of the l^{th} pixel which fit into the n^{th} cluster. Furthermore, p_{nl} desires to fulfil the subsequent limitations,

$$\begin{aligned} \sum_{n=1}^N p_{nl} &= 1, p_{nl} \in [0, 1], \\ 0 &\leq \sum_{l=1}^x p_{nl} \leq x \text{-----} (23) \end{aligned}$$

In equation (1), represents the Euclidean normalization and the factor em ($em > 1$) is act as weight proponent which concludes the overall mass of fuzziness of resultant panel, by Equation (1), the modernize equalities of association degree function p_{nl} which includes the cluster pixilated particles q_n represents by,

$$p_{nl} = \frac{1}{\sum_{k=1}^N (\|a_i - q_n\|^2 / \|a_i - q_k\|^2)^{1/(t-1)}} \text{-----(24)}$$

$$q_n = \frac{\sum_{l=1}^x p_{nl}^t a_i}{\sum_{l=1}^x p_{nl}^t} \text{-----(25)}$$

FCM cluster algorithms including spatial information

D. Spatial Information

To decrease FCMCA's level of sensitivity over noise and other factors in the given image region, there are numerous improved FCMCA algorithms exploits the spatial information resulting by the district window nearby each pixel elements^{7,12-15}. This type of spatial information is specifies native spatial data. The local spatial information consumes had many manifestation procedures. The mean spatial information of the l^{th} pixel can be defined in the subsequent equation. The native local information includes other information like mean spatial information and median spatial information.

$$\psi_l = \frac{1}{|NG_l|} \sum_{p \in NG_l} a_p \text{-----(26)}$$

Such that the set of neighborhood pixels symbolized by NG_l in defined window which focus the pixelated particles at the l^{th} pixel. The cardinality value represents through $|NG_l|$. Likewise, for the l^{th} pixel the median spatial information is articulated by,

$$NG_l = Median\{a_p\}, p \in NG_l$$

Apparently, numerous pixel values holding a relative formation of anhost image. By exploiting the pixels with a comparable distinct neighborhood formation. This type of configuration is called as foreign spatial evidence. For the given l^{th} pixel, the foreign native spatial information \bar{a}_l is figured via,

$$\bar{a}_l = \sum_{m \in T_l^s} T_{lm} a_m \text{-----(27)}$$

In above presented form, T_l^s signifies a $s \times s$ search exploration window positioned at the pixelated particles l^{th} pixel. The foreign spatial value of l^{th} pixel value is calculated by exploiting the given pixels in this frame. T_{lm} ($m \in T_l^s$) is the weightage among the l^{th} and m^{th} pixels, has to fulfill $0 \leq T_{lm} \leq 1$ and $\sum_{m \in T_l^s} T_{lm} = 1$. The factual weight T_{lm} is well-defined by

$$T_{lm} = \frac{1}{DW_l} \exp(-\|a(NC_l) - a(NC_m)\|_{2,\tau}^2 / F^2) \text{-----(28)}$$

In this equation the constant F denotes the filtering degree factor which restricts the deterioration of the weight functional value of T_{lm} , subsequently $DW_l = \sum_{l \in T_l^s} \exp(-\|a(NC_l) - a(NC_m)\|_{2,\tau}^2 / F^2)$ is the normalizing factor. Considerably, this weight value T_{lm} depends on the resemblance among the l^{th} and m^{th} pixels. The significance resemblance is calculated through Gaussian weighted Euclidean distance function $\|a(NC_l) - a(NC_m)\|_{2,\tau}^2$, such that τ ($\tau > 0$) signifies the standard aberration of Gaussian kernel. $a(NC_l)$ is the gray level value vectors within the defined $s \times s$ right-angled neighborhood pixels NC_l pixelated particles at the l^{th} pixel. This is can be formed through equation (8) by which all pixels with a related gray level values of neighboring l^{th} pixel with native larger weights.

E. Merging FCM Cluster Algorithms and Spatial Information

The FCMCA algorithm initially consumes the spatial evident information for every respective pixel value to describe a spatial limitation. The modernized native objective formation will be articulated as,

$$M = \sum_{n=1}^N \sum_{l=1}^x p_{nl}^t \|a_l - q_n\|^2 + \rho \cdot \sum_{n=1}^N \sum_{l=1}^x p_{nl}^t \|\bar{a}_l - q_n\|^2$$

$$= \sum_{n=1}^N \sum_{l=1}^x p_{nl}^t (\|a_l - q_n\|^2 + \rho \cdot \|\bar{a}_l - q_n\|^2) \text{-----(29)}$$

Such \bar{a}_l defines the local spatial evident information otherwise the foreign spatial facts of the l^{th} pixel. In succeeding formula in equation (29) is spatial evident limitation tenure and factual parameter ρ restricts the forfeit consequence. The reduction of equation (29) by Lagrange multiplier scheme produces the subsequent membership

degree parameter. The updated cluster pixelated particles equations can be expressed as,

$$p_{nl} = \frac{1}{\sum_{k=1}^N ((\|a_i - q_n\|^2 + \rho \cdot \|\bar{a}_i - q_n\|^2) / ((\|a_i - q_n\|^2 + \rho \cdot \|\bar{a}_i - q_n\|^2))^{(t-1)})} \quad (30)$$

$$q_n = \frac{\sum_{l=1}^x p_{nl}^t (a_i + \rho \bar{a}_i)}{(1 + \rho) \sum_{l=1}^x p_{nl}^t} \quad (31)$$

5. Proposed Spatial FCM Clustering Algorithm

The pixelated particles representation and dimension initialization with mass value. In FCMCA, each pixelated particles is consumes a factual statistics which characterize the coordinates of the pixelated particles of the each segmentations. If a pixelated particles l encrypts the pixelated particles of N group of defined clusters in D dimensional mass, subsequently the length lenl is occupied as D×N. For instance, a pixelated particle l encrypting four individual cluster pixelated particles s in 3D space is epitomized. Each defined cluster pixelated particles is deliberated to be undividable. Each pixelated particle l in the mass value which encrypts the pixelated particles number Nl of defined clusters, where,

$$N_l = \{rand(\cdot) \bmod (N^{\max} - 1)\} + 2 \quad (32)$$

Such that rand(·) proceeds an arbitrary integer among 0 & ∞, the N^{max} is a concentrated upper part of the total quantity of group clusters. Consequently, amount of group clusters N_l with the range from 2 to N^{max}. In FCMCA, the N_l pixelated particles encrypted in a pixelated particles of the early groups which arbitrarily nominated diverse facts from the given image.

F. Fitness Calculation

In FCMCA, The dualistic fitness functions, such as F_F and F_S are elevated concurrently. F_F is overall density with spatial evident information. F_S denotes the fuzzy set division. Finally the F_F is figured by,

$$F_F = \frac{\sum_{n=1}^N \sum_{l=1}^x P_{nl}^t (\|a_i - q_n\| + \rho \cdot \|\bar{a}_i - q_n\|)}{\sum_{l=1}^x P_{nl}^t} \quad (33)$$

Such that \bar{a}_i represents the foreign native spatial evident information of defined lth pixel value provided ρ is the controlled limitation. The pixelated particles s q₁, q₂, ... , q_N coded in a specified pixelated particles. The determined and the association member degree values p_{nl}, n = 1, 2, ..., N, l = 1, 2, ..., n are computed by, Equation (10).

$$\sum_{l=1}^x P_{nl}^t (\|a_i - q_n\|)$$

Represents the variation of the nth cluster, subsequently,

$$\sum_{l=1}^x P_{nl}^t (\|a_i - q_n\| + \rho \cdot \|\bar{a}_i - q_n\|)$$

Could be deliberated as spatial weighted difference of the nth cluster and represented as $\tau(F_l)$. $\sum_{l=1}^x P_{nl}^t$ in the formation the fuzzy cardinality of defined nth cluster has represented as x_l. Hence, F_F is the overall fuzzy density with spatial data and be exemplified by $F_F = \sum_{n=1}^N \tau F_l / x_l$

If the cluster midpoint q_a is recognized as the midpoint of the given fuzzy set {q_b | 1 ≤ b ≤ N, b ≠ a}, the membership degree value of q_b to q_a is distinct as,

$$\omega_{ab} = \frac{1}{\sum_{k=1, k \neq a}^N ((\|q_b - q_a\|^2) / \|q_b - q_k\|^2)^{1/(t-1)}}, a \neq b \quad (34)$$

$$F_S = \sum_{a=1}^N \sum_{b=1, a \neq b}^N \omega_{ab}^t \|q_b - q_a\|^2 \quad (35)$$



Figure 1. Original host Image.

G. Final Selection by Boundary and Transformation Operation

In FCMCA, packed binary competition selection scheme²⁸ is embraced to produce the copulating group of pixelated particles. In this selection system, formerly the pixelated particles are ordered depends on identical sorting with allocated massive distance parameter, the formation is accomplished by consuming a massive comparative operations²⁸. The crossover sector points could falls amongst two cluster midpoints. Subsequently the crossover process is accomplished stochastically through the crossover likelihood Prob_{CV} and requisite to confirm that descendant's pixelated particles coded as a minimum of dual midpoints. This determination, the crossover operative scheme in equation (30) is incorporated in FCMCA. Presume the native pixelated particles θ_1 and θ_2 and coded N_1 and N_2 cluster midpoints, correspondingly. Consider ϕ_1 be the crossover fact in θ_1 and can be produced as

$$\phi_1 = \text{rand}(\text{mod } N_1)$$

Such that $\text{rand}(\cdot)$ is functionality of rearranging an arbitrary integer among 0 and ∞ . Consider ϕ_2 be the crossover midpoint of N_2 and it might differ in $[L_B(\phi_2), U_B(\phi_2)]$, wherever $L_B(\phi_2)$ and $U_B(\phi_2)$ are the lower and upper boundaries of the series of ϕ_2 , correspondingly. $L_B(\phi_2)$ and $U_B(\phi_2)$ are well-defined as,

$$L_B(\phi_2) = \min[2, \max[0, 2 - (N_1 - \phi_1)]]$$

$$U_B(\phi_2) = [N_2 - \max[0, (2 - \phi_1)]]$$

Consider the case $U_B(\phi_2) \geq L_B(\phi_2)$, ϕ_2 is produced arbitrarily as a numeral among $L_B(\phi_2)$ and $U_B(\phi_2)$. Else $\phi_2 = 0$, this could be effortlessly confirmed. In case if crossover midpoints ϕ_1 and ϕ_2 are selected permitting to the above described rules, formerly the quantity of clusters in every off springs may not decrease to 2. The quantity with clusters sequence is assured on off-springs surpass value N^{max} . Afterwards execution of crossover procedure, the transformation function is functional to pixelated particles. All cluster midpoint coded in a pixelated particles is transformed with the transformation probability Prob_{mu} . However if the N^{th} cluster midpoint P_N requisite to be mutated, then the significance of the a^{th}

dimension of given P_N ($P_{N.a}$) will converts $P_{N.a} \pm 10\zeta$, whereas ζ arbitrary sum with the series of [0,1] having uniform distribution. This signs '+' or '-' ensembles with equal probability.

H. The Absolute Non-Dominated Solution Set

After evaluation of our FCMCA algorithm, it produces a group of unpredictable resolutions are attained. Through algorithmic perspective, all the attained answers were treated with equal importance however the single solution may treated as most accurate and validated properly, So as to accomplish the single solution the new parameter⁴¹ a cluster validity index (CVI) C_{val} has introduced⁴² the C_{val} is simplified as

$$C_{\text{val}} = \left(\frac{1}{N} \times \frac{\exists_1}{\exists_{\text{EU}}} \times \exists_{\text{KE}} \right)$$

Such that N represents the no. of cluster groups. \exists_{EU} & \exists_{KE} are exemplified as,

$$\exists_{\text{EU}} = \sum_{N=1}^N \sum_{l=1}^x p_{nl} \| a_i - q_n \|$$

$$\exists_{\text{KE}} = \max_{a,b=1}^N \| q_b - q_a \|$$

The cluster validity index C_{val} is a structure of three basic aspects, such as $1/N, \exists_1 / \exists_{\text{EU}}, \exists_{\text{KE}} \cdot \exists_{\text{EU}}$ computes the fuzzy density of the data set and minimizes as by N maximizes. This is apparent that \exists_1 is persistent for all defined data set. The \exists_{KE} computes determine parting among any two cluster groups from all cluster groups. The upper constrained by the concentrated parting among any two root points in the given data set. When N is maximized, $1/N$ is minimized, $\exists_1 / \exists_{\text{EU}}$ is maximized and \exists_{KE} is maximized. Therefore these three aspects are originate to compete critical equilibriums. If index C_{val} has larger value which suggests more dense and well-parted cluster groups and specifies improved resolution^{40,41}. More over, the non-local spatial data resultant from the image is familiarized into the index C_{val} and an innovative cluster validity index through spatial information C_{SI} is anticipated to choose the optimum resolution. C_{SI} is simplified as,

$$C_{SI}(N) = \frac{1}{N} \times \frac{\exists_{opt}}{\exists_{opt-ke}} \times \exists_{opt-eu}$$

Such that the calculation of \exists_{opt-eu} is similar to \exists_{KE} , & \exists_{opt-ke} is elaborated as

$$\exists_{opt-ke} = \sum_{n=1}^N \sum_{l=1}^x p_{nl} (\|a_l - q_n\| + \rho \cdot \|\bar{a}_l - q_n\|)$$

From the above equation the membership function p_{nl} is computed via Eq. (10), a_l is well-defined as the non-local spatial data of the l^{th} pixel. The ρ is the spatial controlled factor.

6. Experimental Results and Analysis

To validate the efficiency of FCMCA, certain artificial pictures are utilized in the experimentation and KM⁶, MSFCA¹⁹, FGFCM³⁶, FCM⁴⁰, MOVGA⁴¹, FCM NLS³⁷ are implemented as the proportional approaches. These approaches, FCMCA and MOVGA can inevitably progress the sum of cluster groups sets. The supplementary algorithms are accomplished under diverse quantity of cluster groups stretching from 2 to N^{max} and the final resolution with the maximum value of index C_{val} (Eq.(19)) is deliberated beside with the equivalent quantity of cluster groups sets. In this proposed work, N^{max} is defined as 10 for all the experimentations. Furthermore, the cluster accuracy (CTA)⁴³ and the Adjusted Rand Index (ADRI)⁴⁴ are embraced to assess the robustness of proposed model.

With respect of all the defined methods, except the KM method hold the index value is set to 2. For all the methods the highest iteration number Max_i along with

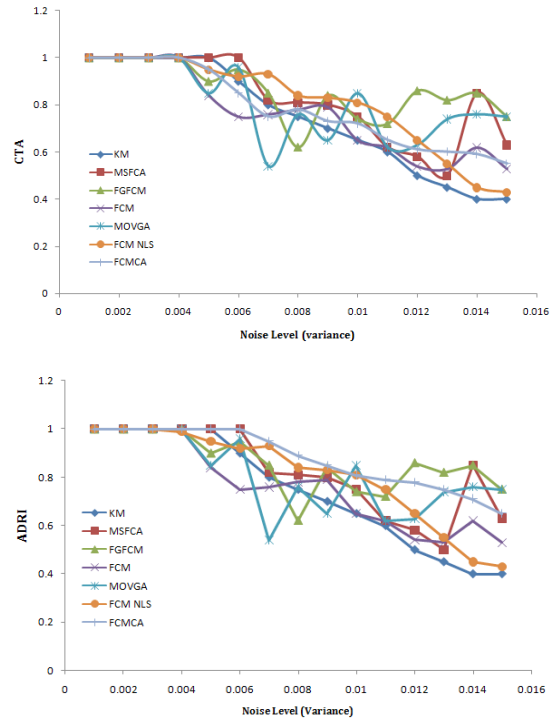
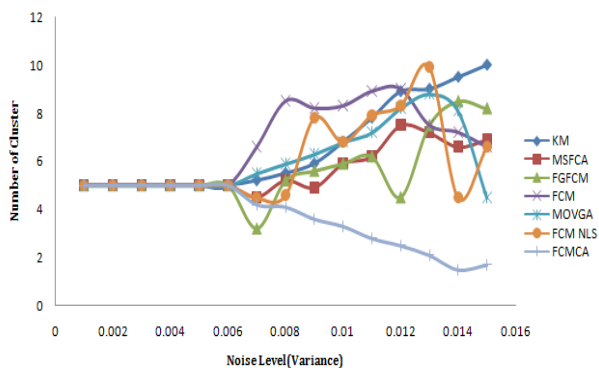


Figure 2. Assessment on performance with other methods. (a) The attained amount of clusters groups; (b) CTA; (c) ADRI.

the stopping threshold value S_{Thres} are set to 350 and 10–6, correspondingly. On other hand the two basic parameters Δ_s and Δ_g of FGFCM method sets to 3 and 6 and these outcomes and investigation are described in the article³⁶. Furthermore from the outcome of FGFCM the neighbor window with the size of 3 x 3 has selected because of its optimality when compared with other methods.

The search window with size of $s \times s$ and the patch with the size of $e \times e$ and the filtering gradation bound F_{ph} for the non-local spatial evidence has clearly discussed in³⁷. By conferring to the investigational examination in³⁷, the factors s , e and F_{ph} are set to 22, 8 and 30. Subsequently the spatial evident factor ρ confines the forfeit penalty consequence and it that has been verified on a set stretching from 0 to 8 in^{28,45}. On other hand Trials in⁴⁵ demonstrations that the segmentation outcomes below $\rho = 6$ are acceptable. At this time, the factor ρ in FCM NLS & FCMCA is fixed to 6. The maximum amount of generation G_{max} and the total population size P_s remain set to 100 to 50 in¹⁸, in the same way it is set to 20 and 20 similarly 40 to 20 in^{40,41}. By widely seeing these comparative situations and algorithm difficulty, the maximum amount

of generation G_{max} and the total the population size P_s with FCMCA and MOVGA are fixed to 40 and 20, correspondingly. In⁴⁰, the crossover probability $Prob_c$ along with the mutation probability $Prob_m$ are fixed to 0.8 & 0.1, individually. Therefore, FCMCA & MOVGA approve the similar value fixing of the factors $Prob_c$ and $Prob_m$.

7. Experiments on Real Image

For this evaluation the real test image with dimension of 100×100 pixels (Figure 1) and it comprises 7 cluster groups with the equivalent gray values as 0, 34, 75, 107, 136, 172 and 217 (Figure 2). In this segment, we make use of this picture along with damaged noise parts along with diverse Gaussian Noise (GN) is to examine the attained amount of cluster groups and divided enactment of FCMCA and proportional procedures. To produce these tainted image sequences, the Gaussian white noise (GWN) with singular mean value of 0 and other normalized modification 0.0003, 0.002, 0.003, 0.005, 0.007, 0.013 and 0.018 is appended to this artificial image, correspondingly.

Figure 3a signifies the attained amount of cluster groups of these approaches on original host images with diverse noise level sequences, and Figures 3b and 3c correspondingly shows that CTA and ADRI bends of these six approaches on defined corrupted images. Figure 2d demonstrations that FCMCA can appropriately progress amount of cluster groups with all noise stages. The cluster value of KM, FCM NLS, FCM and FGFCM conforming to the maximum significance of index C_{val} are accurate. Although the FCM, attained amount of cluster groups lesser noise level with mean of 0 and variance 0.007 is right, the equivalent CTA and ADRI standards are unacceptable, which are presented in Figure 2b and c. The FCMCA attains the maximum CTA and ADRI standards underneath to entire noise levels excluding the final noise level. Consequently, further down the most noise levels, FCMCA performs fine in developing the precise amount of cluster groups and attaining acceptable CTA and ADRI values. Figure 3 illustrates the corrupted artificial image with Gaussian white noise with zero mean value and standardized variance value 0.013. This could be originate from Figure 3a that merely FCMCA amongst all the approaches can perceive the amount of cluster groups on this noise corrupted picture. The equivalent segmentation outcomes of these approaches are offered in Figures

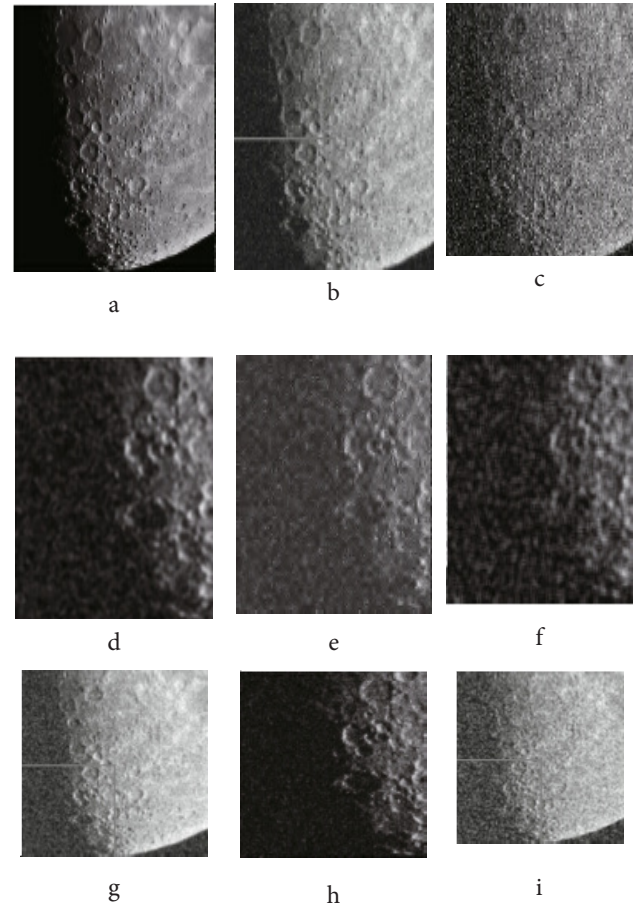


Figure 3. Segmentation outcomes on host image #23895100 corrupted by the GN (0, 0.01): (a) Host image; (b) Comparative benchmark image; (c) Cluttered and noisy image; (d) KM; (e) MSFCA; (f) FGFCM (g) FCM;; (h) MOVGA; (i) FCMCA.

3b–g. These outcomes disclose that FCMCA is the finest amongst all the approaches even if the actual amount of cluster groups is assumed for the additional approaches.

8. Conclusion

The proposed FCMCA model for effective image segmentation is to improve agility and performance of conventional FCM clustering technique on noisy images, FCMCA commences effective foreign spatial evident information via the noisy image and transform into robustness. Furthermore, the foreign spatial evidence is also initiated into CVI through the best possible resolutions. The appropriateness and CVI through foreign spatial evidence could conquer the impact of noisy image

into the grouping concert. In this process a variable length string technique is emphasized. The evaluation outcomes on the images shows dynamism on FCMCA, as a result of the non-linearity of the energy fitness function, conventional scheme by proving EL equation is tend to reduce the energy consumption. This reflects in lower conjunction rapidity with our proposed system by comparing with KM, MSFCA, FGFCM, FCM, MOVGA and FCM NLS. It is recognized that the appropriateness is the critical important characteristic for FCM clustering algorithm. The performance of an algorithm is rectifies the superior influence level of noisy image; our prospect work comprises few additional effectual image spatial information hooked on to refine fitness functions. Additionally, our potential future investigation furthermore incorporate by utilizing two other factors edge and region which is consequent since the noisy host image to build final fitness calculations.

9. References

1. Patra S, Gautam R, Singla A. A novel context sensitive multilevel thresholding for image segmentation, *Appl. Soft Comput.* 2014; 23(12):2–127.
2. Ji Z, Xia Y, Chen Q, Sun Q, Xia D, Feng DD. Fuzzy c-means clustering with weighted image patch for image segmentation. *Appl. Soft Comput.* 2012; 12(6):1659–67.
3. Caselles V, Kimmel R, Sapiro G. Geodesic active contours. *Int. J. Comput. Vis.* 1997; 22(1):61–79.
4. Chen Y, Tagare HD, Thiruvankadam S, Huang F, Wilson D, Gopinath KS, Briggs RW, Geiser EA. Using prior shapes in geometric active contours in a variational framework. *Int. J. Comput. Vis.* 2002; 50(3):315–28.
5. Yang, Gao X, Li J, Han B. A shape-initialized and intensity-adaptive level set method for auroral oval segmentation. *Inf. Sci.* 2014; 277:794–807.
6. Balla-Arabe S, Gao X, Wang B. A fast and robust level set method for image segmentation using fuzzy clustering and lattice Boltzmann method. *IEEE Trans. Cybern.* 2013; 43(3):910–20.
7. Kass M, Witkin A, Terzopoulos D. Snakes: active contour models. *Int. J. Comput. Vis.* 1988; 1(4):321–31.
8. Xu C, Prince JL. Snakes, shapes, and gradient vector flow. *IEEE Trans. Image Process.* 1998; 7(March(3)):359–69.
9. Li C, Xu C, Gui C, Fox MD. Level set evolution without re-initialization: a new variational formulation. In: *IEEE Conference on Computer Vision and Pattern Recognition.* 2005; 1:430–36.
10. Li C, Xu C, Gui C, Fox MD. Distance regularized level set evolution and its application to image segmentation. *IEEE Trans. Image Process.* 2010; 19 (December(12)):3243–54.
11. Chan TF, Vese LA. Active contours without edges. *IEEE Trans. Image Process.* 2001; 10(February(2)):266–77.
12. Li C, Kao C, Gore JC, Ding Z. Minimization of region-scalable fitting energy for image segmentation. *IEEE Trans. Image Process.* 2008; 17(October(10)):1940–49.
13. Li C, Kao C, Gore JC, Ding Z. Implicit active contours driven by local binary fitting energy. In: *IEEE Conference on Computer Vision and Pattern Recognition.* 2007; p. 1–7.
14. Bertelli L, Sumengen B, Manjunath B, Gibou F. A variational framework for multi region pairwise-similarity-based image segmentation. *IEEE Trans. Pattern Anal. Mach. Intell.* 2008; 30(August(8)):1400–14.
15. Mumford D, Shah J. Optimal approximations by piecewise smooth functions and associated variational problems. *Commun. Pure Appl. Math.* 1989; 42:577–685.
16. Osher S, Fedkiw R. New York: Springer-Verlag: *Level Set Methods and Dynamic Implicit Surfaces.* 2003.
17. Sussman M, Smereka P, Osher S. A level set approach for computing solutions to incompressible two-phase flow. *J. Comput. Phys.* 1994; 114(1):146–59.
18. Gomes J, Faugeras O. Reconciling distance functions and level sets. *J. Visual Commun. Image Represent.* 2000; 11(2):209–23.
19. Brown ES, Chan TF, Bresson X. Completely convex formulation of the Chan–Vese image segmentation model. *Int. J. Comput. Vis.* 2012; 98(1):103–21.
20. Gong M, Tian D, Su L, Jiao L. An efficient bi-convex fuzzy variational image segmentation method. *Inf. Sci.* 2015; 293:351–69.
21. Krinidis S, Chatzis V. Fuzzy energy-based active contours. *IEEE Trans. Image Process.* 2009; 18(December(12)):2747–55.
22. Song B, Chan T. A Fast Algorithm for Level Set based Optimization. *UCLA CamReport.* 2002; 2:68–76.
23. Ganesan P, Rajini V, Sathish BS, Kalist V, Khamar Basha SK. Satellite Image Segmentation Based on YcbCr Color Space. *Indian Journal of Science and Technology.* 2015 Jan; 8(1). Doi: 10.17485/ijst/2015/v8i1/51281.
24. Sujatha P, Sudha KK. Performance Analysis of Different Edge Detection Techniques for Image Segmentation. *Indian Journal of Science and Technology.* 2015 July; 8(14). Doi: 10.17485/ijst/2015/v8i14/72946.
25. Otsu N. A threshold selection method from gray-level histograms. *IEEE Trans. Syst. Man Cybern.* 1979; 9(1):62–66.
26. Kumar Rajiv, Arthanariee AM. Performance Evaluation and Comparative Analysis of Proposed Image Segmentation Algorithm. *Indian Journal of Science and Technology.* 2014 Jan; 7(1). Doi: 10.17485/ijst/2014/v7i1/46678.

27. Nookala Venu, Anuradha B. Multi-Kernels Integration for FCM Algorithm for Medical Image Segmentation using Histogram Analysis. *Indian Journal of Science and Technology*. 2015 Dec; 8(34). Doi: 10.17485/ijst/2015/v8i34/72409.
28. Mahalakshmi S, Velmurugan T. Detection of Brain Tumor by Particle Swarm Optimization using Image Segmentation. *Indian Journal of Science and Technology*. 2015 Sep; 8(22). Doi: 10.17485/ijst/2015/v8i22/79092.
29. Caldairoua B, Passata N, Habas PA, Studholme C, Rousseau F. A non-local fuzzy segmentation method: application to brain MRI. *Pattern Recognit*. 2010; 44(9):1916–27.
30. Hojjatoleslami SA, Kittler J. Region growing: a new approach. *IEEE Trans. Image Process*. 1998; 7(7):1079–84.
31. Haris K, Efstratiadis SN, Maglaveras N, Katsaggelos AK. Hybrid image segmentation using watersheds and fast region merging. *IEEE Trans. ImageProcess*. 1998; 7(12):1684–99.
32. Sowmya B, Sheela Rani B. Colour image segmentation using fuzzy clustering techniques and competitive neural network. *Appl. Soft Comput*. 2011; 11(3):3170–78.
33. Ahmed MN, Yamany SM, Mohamed N, Farag AA, Moriarty T. A modified fuzzy c-means algorithm for bias field estimation and segmentation of MRI data. *IEEE Trans. Med. Imaging*. 2002; 21(3):193–99.
34. Szilagyi L, Benyo Z, Szilagyi S, Adam HS. MR brain image segmentation using an enhanced fuzzy c-means algorithm. In: *Proceedings of 25th Annual International Conference of the IEEE Engineering in Medicine and Biology Society*. 2003; 1:724–26.
35. Zhang DQ, Chen SC. A novel kernelized fuzzy c-means algorithm with application in medical image segmentation. *Artif. Intell. Med*. 2004; 32(1):37–50.
36. Cai W, Chen SC, Zhang DQ. Fast and robust fuzzy c-means clustering algorithms incorporating local information for image segmentation. *Pattern Recognit*. 2007; 40(3):825–38.
37. Zhao F, Jiao LC, Liu HQ. Fuzzy c-means clustering with non-local spatial information for noisy image segmentation. *Front. Comput. Sci. China*. 2011; 5:45–56.
38. Premaladha J, Lakshmi Priya M, Sujitha S, Ravichandran KS. A Survey on Color Image Segmentation Techniques for Melanoma Diagnosis. *Indian Journal of Science and Technology*. 2015 Sep; 8(22). Doi: 10.17485/ijst/2015/v8i22/79192.
39. Loganathan R, Kumaraswamy YS. Active Contour Based Medical Image Segmentation and Compression using Biorthogonal Wavelet and Embedded Zerotree. *Indian Journal of Science and Technology*. 2013 Apr; 6(4). Doi: 10.17485/ijst/2013/v6i4/31870.
40. Yang DD, Jiao LC, Gong MG, Liu F. Artificial immune multi-objective SAR image segmentation with fused complementary features. *Inf. Sci*. 2011; 181(13):2797–812.
41. Mukhopadhyay, Maulik U. A multiobjective approach to MR brain image segmentation. *Appl. Soft Comput*. 2011; 11(1):872–80.
42. Maulik U, Bandyopadhyay S. Performance evaluation of some clustering algorithms and validity indices. *IEEE Trans. Pattern Anal. Mach. Intell*. 2002; 24(12):1650–54.
43. Wu M, Scholkopf B. A local learning approach for clustering. In: *Advances in Neural Information Processing Systems*. 2007; 1529–36.
44. Yeung KY, Ruzzo WL. An empirical study on principal component analysis for clustering gene expression data. *Bioinformatics*. 2001; 17(9):763–74.
45. Zhao F, Jiao LC, Liu HQ. Kernel generalized fuzzy c-means clustering with spatial information for image segmentation. *Digital Signal Process*. 2013; 23(1):184–99.
46. Zhaoa Feng, Hanqiang Liub, Jiulun Fana. A multiobjective spatial fuzzy clustering algorithm for image segmentation. *Applied Soft Computing*. 2015; 30:48–57.